

## Lehigh University Lehigh Preserve

---

Fritz Laboratory Reports

Civil and Environmental Engineering

---

1973

# On slip surface and slope stability analysis, September 1973 (75-36)

Nimitchai Snitbhan

Wai-Fah Chen

Follow this and additional works at: <http://preserve.lehigh.edu/engr-civil-environmental-fritz-lab-reports>

---

### Recommended Citation

Snitbhan, Nimitchai and Chen, Wai-Fah, "On slip surface and slope stability analysis, September 1973 (75-36)" (1973). *Fritz Laboratory Reports*. Paper 1988.

<http://preserve.lehigh.edu/engr-civil-environmental-fritz-lab-reports/1988>

This Technical Report is brought to you for free and open access by the Civil and Environmental Engineering at Lehigh Preserve. It has been accepted for inclusion in Fritz Laboratory Reports by an authorized administrator of Lehigh Preserve. For more information, please contact [preserve@lehigh.edu](mailto:preserve@lehigh.edu).

ON SLIP SURFACE AND  
SLOPE STABILITY ANALYSIS

by  
Nimitchai Snitbhan  
Wai F. Chen

Fritz Engineering Laboratory  
Department of Civil Engineering  
Lehigh University  
Bethlehem, Pennsylvania

September 1973

Fritz Engineering Laboratory Report No. 355.17

# ON SLIP SURFACE AND SLOPE STABILITY ANALYSIS

by

N. Snitbhan<sup>1</sup> and W. F. Chen<sup>2</sup>

## ABSTRACT

Key Words: normal stress distribution; slip surface; slope stability;  
soil mechanics; variational method

The method of variational calculus is applied to obtain the shape of slip surface and the corresponding normal stress distribution. For a horizontal slope of uniform soil, a logarithmic spiral surface of angle  $\phi$  is found to be the most critical surface. This contradicts the report made earlier by Spencer. The results also emphasize the correctness of the log-spiral failure mechanism assumed in the upper bound method of limit analysis.

---

<sup>1</sup>Grad. Student, Dept. of Civ. Engrg., Lehigh Univ., Bethlehem, Pa.; formerly Design Engineer, Fuller Company, Catasauqua, Pa.

<sup>2</sup>Associate Prof. of Civ. Engrg., Fritz Lab., Lehigh Univ., Bethlehem, Pa.

## TABLE OF CONTENTS

	<u>Page</u>
ABSTRACT	i
1. INTRODUCTION	1
2. SOME PHYSICAL FACTS AND THEIR SIGNIFICANCE	2
3. MATHEMATICAL FORMULATION OF THE PROBLEM	3
4. SHAPE OF SLIP SURFACE	6
5. NORMAL STRESS DISTRIBUTION	7
6. CONCLUSIONS	8
7. ACKNOWLEDGEMENTS	9
APPENDIX I - REFERENCES	10
APPENDIX II	11
APPENDIX III - NOTATION	13
FIGURES	14

## 1. INTRODUCTION

In the recent work of Spencer [5] on the shape of slip surface in the stability analysis of embankments in uniform soil, the following two questions were raised:

1. Is the arc of a logarithmic spiral a more critical shape for the cross-section of the slip surface than a circular arc?
2. If the slip surface is an arc of a logarithmic spiral in cross-section, is its shape determined by the angle of shearing resistance  $\phi$  of the soil?

To answer these questions, Spencer analyzed the problem using the method of slices with the assumption of parallel interslice forces and concluded that (1) the circular slip surface is more critical than the logarithmic spiral; and (2) there is no justification for assuming that the shape of the spiral is determined by the value of the angle of internal friction  $\phi$  of soil.

In a follow-up discussion to the paper, Chen [1] pointed out that the shape of slip surface and the normal stress distribution are interrelated and both factors should be treated as the variables. By assuming that the interslice forces being parallel to each other in the method of slices, the variable on the normal stress distribution for different shapes of slip surface was being implicitly assumed in Spencer's analysis. Chen concluded that the proper method of analysis to answer the above mentioned questions should therefore consider all the shapes of the slip surfaces as well as all the possible distribution

of normal stress on the slip surface. Chen, although disagreed with Spencer's conclusion, did not present any analytical results of establishing the most critical slip surface and its associated normal stress distribution on the surface. However, Chen did suggest that this is an optimization problem and can be approached by applying the method of calculus of variations. The method may require considerable mathematical treatment to arrive at any appreciable solution.

The work to be described herein is directed towards an attempt to settle this argument. Using the method of variational calculus, the shape and normal stress distribution of the most critical surface are determined simultaneously.

It may be of interest to note that, by using the log-spiral surface of angle  $\phi$ , the moment equation of static equilibrium is independent of the normal stress distribution along the surface and, thus, permits the stability problems to be solved in a relatively simple mathematical form.

## 2. SOME PHYSICAL FACTS AND THEIR SIGNIFICANCE

A typical slope of homogenous soil under a uniform surcharge load,  $q$  is shown in Fig. 1. The slope remains stable as long as the stress developed within the soil mass does not exceed soil strength. Instability is initiated as the applied load  $q$  reaches its critical value and the collapse of the slope may be described by the rigid body slide of soil mass along one of many "potential" surfaces,  $S_n$  as shown in Fig. 1. At the incipient of collapse, the conditions of static

equilibrium of the sliding mass

$$\Sigma H = 0, \quad \Sigma V = 0, \quad \Sigma M = 0 \quad (1)$$

as well as the yield or failure criterion must be satisfied everywhere along the surface. The most critical of all these potential surfaces is theoretically the one which allows minimum applied load. In absence of surcharge load ( $q = 0$ ), the gravitational weight of the soil mass acts solely as the external load applied on the slope.

As an example, consider a uniform slope of Fig. 2. The positions and values of stability factors,  $N_s = H_c \gamma / c$  for several critical slip surfaces (plane, circular and log-spiral) have been given by Taylor [7] where  $H_c$  = critical height,  $c$  = cohesion and  $\gamma$  = unit weight. It is possible, then, to sketch in one figure the three types of slip surfaces and compare the volume of the sliding mass for each surface. This is illustrated in Fig. 3 for slopes having base angles of  $\beta = 90^\circ$  and  $\beta = 70^\circ$ . The results show clearly that the most critical shape is the log-spiral surface which also corresponds to the minimum weight  $W$  of the sliding mass. It can, therefore, be concluded that, of all the potential slip surfaces, the one which allows the minimum weight  $W$  of the sliding mass gives the most critical situation. This condition will be used as the criterion of optimization in the following mathematical formulation.

### 3. MATHEMATICAL FORMULATION OF THE PROBLEM

As stated earlier, in absence of load  $q$  the weight of the sliding mass  $W$  is the only applied load on slope and may be defined

by a functional

$$W = \int_s P_w d\theta \quad (2)$$

$$P_w = \frac{\gamma r^2}{2} - W_1 / (\theta_h - \theta_o) \quad (3)$$

in which  $W_1$  is weight of the area O-B-A-C as shown in Fig. 2 and  $r(\theta)$  is an unknown function defining the shape of the slip surface.

Referring to Eq. 1 and Fig. 2, the three equilibrium equations can be written as

$\Sigma$  horizontal forces = 0 gives

$$\int_s [\tau \cos\alpha - \sigma \sin\alpha] ds = 0 \quad (4)$$

$\Sigma$  vertical forces = 0 gives

$$\int_s [-\tau \sin\alpha - \sigma \cos\alpha] ds + W = 0 \quad (5)$$

$\Sigma$  moment = 0 gives

$$\int_s [\sigma r \sin\xi - \tau r \cos\xi] ds + W l = 0 \quad (6)$$

$$\alpha = \pi - \theta - \arctan\left(\frac{r}{r'}\right) \quad (7a)$$

$$\xi = \frac{\pi}{2} - \arctan\left(\frac{r}{r'}\right) \quad (7b)$$

The tangential shear stress,  $\tau$  and normal stress,  $\sigma$  are related through the following Coulomb failure or yield criterion

$$\tau = c + \sigma \tan\phi \quad (8)$$

Using the Coulomb criterion (8), Eqs. 4, 5 and 6 become

$$\int_{\theta_o}^{\theta_h} P_1 d\theta = 0, \quad \int_{\theta_o}^{\theta_h} P_2 d\theta = 0, \quad \int_{\theta_o}^{\theta_h} P_3 d\theta = 0 \quad (9a,b,c)$$



in which

$$P_1 = (-\sigma) \left[ (r \cos\theta)' \tan\varphi + (r \sin\theta)' \right] - c(r \cos\theta)' \quad (10)$$

$$P_2 = \sigma \left[ (r \cos\theta)' - (r \sin\theta)' \tan\varphi \right] - c(r \sin\theta)' \quad (11)$$

$$+ \frac{\gamma}{2} r^2 - \frac{W_1}{\theta_h - \theta_o}$$

$$P_3 = \sigma (rr' - r^2 \tan\varphi) - c r^2 + \frac{\gamma}{3} r^3 \cos\theta - \frac{W_1 \ell_1}{\theta_h - \theta_o} \quad (12)$$

where  $r(\theta)$  and  $\sigma(\theta)$  are as yet two unknown functions. The problem of finding the critical slip surface and its associated normal stress distribution on the surface may now be stated as follows: Given the slope shown in Fig. 2, determine the shape function  $r(\theta)$  and stress function  $\sigma(\theta)$  so as to minimize the weight functional,  $W$  of Eq. 2 subjected to the constraint conditions of equations (9a,b,c). With Lagrange's multiplier denoted by  $\lambda_1$ ,  $\lambda_2$  and  $\lambda_3$ , one can write

$$I = P_w + \lambda_1 P_1 + \lambda_2 P_2 + \lambda_3 P_3 \quad (13)$$

Since all integrands in  $P_w$ ,  $P_1$ ,  $P_2$  and  $P_3$  involve only  $r(\theta)$ ,  $\sigma(\theta)$  and the first derivative of  $r(\theta)$ , the Euler differential equation will be first order, and can be represented by

$$\frac{d}{d\theta} \left[ \frac{\partial I}{\partial \sigma'(\theta)} \right] - \frac{\partial I}{\partial \sigma(\theta)} = 0 \quad (14)$$

and

$$\frac{d}{d\theta} \left[ \frac{\partial I}{\partial r'(\theta)} \right] - \frac{\partial I}{\partial r(\theta)} = 0 \quad (15)$$

After substitution, integration and simplification of equations (14,15), it follows that the two unknown functions  $r(\theta)$  and  $\sigma(\theta)$  must satisfy the following first-order differential equations

$$\begin{aligned}
& r' \left[ \lambda_2 (\cos\theta - \tan\varphi \sin\theta) - \lambda_1 (\tan\varphi \cos\theta + \sin\theta) \right] \\
& + r \left[ \lambda_1 (\tan\varphi \sin\theta - \cos\theta) - \lambda_2 (\sin\theta + \tan\varphi \cos\theta) \right] \\
& + (rr' - r^2 \tan\varphi) \lambda_3 = 0
\end{aligned} \tag{16}$$

independently of the normal stress distribution  $\sigma(\theta)$ , and

$$\begin{aligned}
& \sigma' \left[ \lambda_2 (\cos\theta - \tan\varphi \sin\theta) - \lambda_1 (\tan\varphi \cos\theta + \sin\theta) + \lambda_3 r \right] \\
& + \sigma (2r \lambda_3 \tan\varphi) - \gamma r (1 + \lambda_2) + \lambda_3 (2c r - \gamma r^2 \cos\theta) = 0
\end{aligned} \tag{17}$$

The shape of the most critical slip surface can therefore be obtained by first solving Eq. 16 for  $r(\theta)$ . Once the function  $r(\theta)$  is determined Eq. 17 can then be used for the determination of  $\sigma(\theta)$  which describes the corresponding normal stress distribution along the critical slip surface obtained earlier.

#### 4. SHAPE OF SLIP SURFACE

For convenience of solution, Eq. 16 is now transformed from polar to cartesian coordinates (Fig. 4)

$$\begin{aligned}
& \lambda_1 y' - \lambda_2 - \lambda_3 (yy' + x) \\
& + \tan\varphi \left[ \lambda_1 + \lambda_2 y' - \lambda_3 (y - xy') \right] = 0
\end{aligned} \tag{18}$$

where  $x = r \cos\theta$ ,  $y = r \sin\theta$

Equation (18) can also be written in the form

$$- y' \left( y - \frac{\lambda_1}{\lambda_3} \right) - \left( x + \frac{\lambda_2}{\lambda_3} \right) + \tan\varphi \left[ - \left( y - \frac{\lambda_1}{\lambda_3} \right) + y' \left( x + \frac{\lambda_2}{\lambda_3} \right) \right] = 0 \tag{19}$$

Let

$$X = x + \frac{\lambda_2}{\lambda_3}, \quad Y = y - \frac{\lambda_1}{\lambda_3} \quad (20)$$

Equation (19) now becomes

$$- Y'Y - X + \tan\varphi(- Y + Y'X) = 0 \quad (21)$$

By substitution into Eq. 21 the following terms

$$X = \bar{r} \cos\bar{\theta}, \quad Y = \bar{r} \sin\bar{\theta}$$

$$Y' = \frac{\bar{r} \cos\bar{\theta} + \bar{r}' \sin\bar{\theta}}{\bar{r}' \cos\bar{\theta} - \bar{r} \sin\bar{\theta}}$$

the complicate form of Eq. 16 now reduces to the simple form

$$\bar{r}^2 \tan\varphi - \bar{r} \bar{r}' = 0 \quad (22)$$

from which

$$\bar{r}(\bar{\theta}) = \bar{r}_0 \exp(\bar{\theta} - \bar{\theta}_0) \tan\varphi \quad (23)$$

is the general solution. Equation (23) obviously represents the simplest form of log-spiral surface of angle  $\varphi$  having  $\bar{r}_0$  as an arbitrary constant.

## 5. NORMAL STRESS DISTRIBUTION

Rewriting Eq. 17 with respect to the new coordinates, one obtains

$$\sigma' + 2 \sigma \tan\varphi - \frac{Y}{\lambda_3} + 2c - \gamma \bar{r} \cos\bar{\theta} = 0 \quad (24)$$

Equation (24) is a linear, first-order differential equation from which there exists an exact solution of the form

$$\sigma(\bar{\theta}) = \frac{\gamma}{2 \lambda_3 \tan \varphi} - \frac{c}{\tan \varphi} + \frac{\gamma \bar{r}_0 \exp(\bar{\theta} - \bar{\theta}_0) \tan \varphi}{1 + 9 \tan^2 \varphi}$$

$$(3 \tan \varphi \cos \bar{\theta} + \sin \bar{\theta}) + D \exp(-2 \bar{\theta} \tan \varphi) \quad (25)$$

in which the Lagrange multiplier,  $\lambda_3$  and the integration constant,  $D$  are as yet to be determined.

Since the moment equation (9c) is independent of  $\sigma(\bar{\theta})$ , the two remaining force equations (9a,b) may therefore be satisfied by the proper choices of  $\lambda_3$  and  $D$ . Substitute  $\bar{r}(\bar{\theta})$  of Eq. 23 and  $\sigma(\bar{\theta})$  of Eq. 25 into Eqs. 9a,b and solve for  $\lambda_3$  and  $D$ , the final form of the non-dimensionalized  $\sigma(\bar{\theta})$  can be expressed by

$$\frac{\sigma(\bar{\theta})}{\gamma H} = A_1 + \left[ \frac{3 \tan \varphi}{(H/\bar{r}_0) (1 + 9 \tan^2 \varphi) \exp(\bar{\theta}_0 \tan \varphi)} \right]$$

$$\left[ \cos \bar{\theta} \exp(\bar{\theta} \tan \varphi) + \frac{\sin \bar{\theta} \exp(\bar{\theta} \tan \varphi)}{3 \tan \varphi} \right] + A_2 \exp(-2 \bar{\theta} \tan \varphi) \quad (26)$$

The constant terms of  $A_1$ ,  $A_2$  and  $H/\bar{r}_0$  are given in details in Appendix II. As an illustration, Fig. 5 shows the normal stress distribution obtained from Eq. 26, for slopes with base angles of  $\beta = 90^\circ$  and  $\beta = 70^\circ$  and soil friction angle  $\varphi = 20^\circ$ .

## 6. CONCLUSIONS

From the results of this work, the following conclusions can be drawn:

1. For a horizontal slope of uniform soil, the most critical slip surface is logarithmic spiral of angle  $\varphi$ .

2. The normal stress distribution is not generally independent of the shape of slip surface. Although any assumed normal stress distribution in the conventional methods of analysis may give a reasonable answer, it does not always lead to the optimum solution.
3. The rotational failure mechanism (logarithmic spiral) utilized in the upper bound method of limit analysis is appropriate in the framework of limit equilibrium methods. The results reported in Ref. [2] should therefore present the best possible solution of the problem.
4. The variational method provides a profound and useful means of analyzing slope stability problems. For the case of complicate slope boundary and loading conditions, the mathematical formulation of the problem with proper modifications is still applicable and the numerical results can always be obtained without much difficulties.

#### 7. ACKNOWLEDGEMENTS

The research reported herein was supported by the National Science Foundation under Grant GK-14274 to Lehigh University.

Many helpful suggestions made by Dr. H. Y. Fang, Director of Geotechnical Division, and Dr. D. Edelen of the Center for the Application of Mathematics are gratefully acknowledged.

The writers thank Shirley Matlock for typing the manuscript and John Gera for the figure drafting.

APPENDIX I - REFERENCES

1. Chen, W. F.  
DISCUSSION ON CIRCULAR AND LOGARITHMIC SPIRAL SLIP SURFACES,  
Journal of Soil Mechanics and Foundations Division, ASCE,  
Vol. 96, No. SM1, January 1970, pp. 324-326.
2. Chen, W. F., Snitbhan, N. and Fang, H. Y.  
STABILITY OF SLOPES IN ANISOTROPIC NONHOMOGENEOUS SOILS,  
Fritz Engineering Laboratory Report No. 355.13, Lehigh  
University, Bethlehem, Pa., March 1972.
3. Hilderbrand, F. B.  
METHODS OF APPLIED MATHEMATICS, Second Edition, Prentice-Hall,  
Inc., Englewood Cliffs, New Jersey, pp. 119-193.
4. Kogan, B. I., and Lupashko, A. A.  
STABILITY ANALYSIS OF SLOPES, Soil Mechanics and Foundation  
Engineering, No. 3, May-June 1970, pp. 153-157.
5. Spencer, E.  
CIRCULAR AND LOGARITHMIC SPIRAL SLIP SURFACES, Journal of  
Soil Mechanics and Foundations Division, ASCE, Vol. 95,  
No. SM1, January 1969, pp. 227-234.
6. Spencer, E.  
CLOSURE ON CIRCULAR AND LOGARITHMIC SPIRAL SLIP SURFACES,  
Journal of Soil Mechanics and Foundations Division, ASCE,  
Vol. 96, No. SM4, July 1970, pp. 1466-1467.
7. Taylor, D. W.  
FUNDAMENTALS OF SOIL MECHANICS, John Wiley and Sons, New  
York, 1948.

APPENDIX II

The following are constant terms which must be substituted into Eq. 26 to obtain the required normal stress distribution  $\sigma(\theta)$  in its non-dimensionalized form.

$$\begin{aligned}
 A_1 = & \frac{1}{\frac{u_3(\theta) \Big|_{\theta_o}^{\theta_h}}{u_3(-\theta) \Big|_{\theta_o}^{\theta_h}} + \frac{u_1(\theta) \Big|_{\theta_o}^{\theta_h}}{u_1(-\theta) \Big|_{\theta_o}^{\theta_h}}} \left\{ \frac{[-3(1 + \tan^2\varphi) u_4(2\theta) - 3\tan\varphi u_1(2\theta) - u_3(2\theta)] \theta_o^{\theta_h}}{4(H/r_o) (1 + 9\tan^2\varphi) u_4(\theta_o) u_1(-\theta) \Big|_{\theta_o}^{\theta_h}} \right. \\
 & + \frac{(\cos\varphi + 17\tan\varphi) u_4(2\theta) \Big|_{\theta_o}^{\theta_h} + u_1(2\theta) \Big|_{\theta_o}^{\theta_h} - 3\tan\varphi u_3(2\theta) \Big|_{\theta_o}^{\theta_h}}{4(H/r_o) (1 + 9\tan^2\varphi) u_4(\theta_o) u_3(-\theta) \Big|_{\theta_o}^{\theta_h}} \\
 & - \frac{[\tan\varphi u_1(\theta) - u_3(\theta)] \theta_o^{\theta_h}}{f(1 + \tan^2\varphi) u_1(-\theta) \Big|_{\theta_o}^{\theta_h}} - \frac{[u_1(\theta) + \tan\varphi u_3(\theta)] \theta_o^{\theta_h}}{f(1 + \tan^2\varphi) u_3(-\theta) \Big|_{\theta_o}^{\theta_h}} \\
 & - \frac{(L/r_o) \sin\theta_o u_4(\theta_o) - [\sin\theta_h \cos\theta_o + (L/r_o) \sin\theta_h - \sin\theta_o \cos\theta_h] u_4(\theta_h)}{2(H/r_o) u_3(-\theta) \Big|_{\theta_o}^{\theta_h}} \\
 A_2 = & \frac{[\tan\varphi u_1(\theta) - u_3(\theta)] \theta_o^{\theta_h}}{f(1 + \tan^2\varphi) u_1(-\theta) \Big|_{\theta_o}^{\theta_h}} - \frac{u_1(\theta) \Big|_{\theta_o}^{\theta_h}}{u_1(-\theta) \Big|_{\theta_o}^{\theta_h}} (A_1) \\
 & - \frac{[3(1 + \tan^2\varphi) u_4(2\theta) + 3\tan\varphi u_1(2\theta) + u_3(2\theta)] \theta_o^{\theta_h}}{4(H/r_o) (1 + 9\tan^2\varphi) u_4(\theta_o) u_1(-\theta) \Big|_{\theta_o}^{\theta_h}}
 \end{aligned}$$

where the functions  $u(\theta)$  and  $f$  are defined as

$$u_1(\theta) = (\tan\varphi \cos\theta + \sin\theta) \exp(\theta \tan\varphi)$$

$$u_2(\theta) = (\tan\varphi \sin\theta + \cos\theta) \exp(\theta \tan\varphi)$$

$$u_3(\theta) = (\tan\varphi \sin\theta - \cos\theta) \exp(\theta \tan\varphi)$$

$$u_4(\theta) = \exp(\theta \tan\varphi)$$

$$f = \left\{ \frac{\exp[2(\theta_h - \theta_o) \tan\varphi] - 1}{2 \tan\varphi (f_1 - f_2 - f_3)} \right\} \left\{ \sin\theta_h \exp[(\theta_h - \theta_o) \tan\varphi] - \sin\theta_o \right\}$$

$$f_1 = \frac{1}{3(1 + 9 \tan^2\varphi)} \left\{ (3 \tan\varphi \cos\theta_h + \sin\theta_h) \exp[3(\theta_h - \theta_o) \tan\varphi] - (3 \tan\varphi \cos\theta_o + \sin\theta_o) \right\}$$

$$f_2 = \frac{\sin\theta_o (L/r_o) (2 \cos\theta_o - L/r_o)}{6}$$

$$f_3 = \frac{\exp[(\theta_h - \theta_o) \tan\varphi]}{6} \left[ \sin(\theta_h - \theta_o) - (L/r_o) \sin\theta_h \right] \left\{ \cos\theta_o - (L/r_o) + \cos\theta_h \exp[(\theta_h - \theta_o) \tan\varphi] \right\}$$

and the ratios  $H/r_o$  and  $L/r_o$  can be expressed in terms of the angles  $\theta_o$  and  $\theta_h$  in the forms

$$H/r_o = \sin\theta_h \exp[(\theta_h - \theta_o) \tan\varphi] - \sin\theta_o$$

and

$$L/r_o = \cos\theta_o - (H/r_o) \cot\beta - \cos\theta_h \exp[(\theta_h - \theta_o) \tan\varphi]$$



APPENDIX III - NOTATION

The following symbols are used in this paper.

$A_1, A_2$	= constants defined in Appendix II
$c$	= cohesion
$D$	= integration constant in Eq. 25
$f, f_1, f_2, f_3$	= functions defined in Appendix II
$H, H_c$	= height and critical height of embankment, respectively
$I$	= function defined in Eq. 13
$L$	= length, see Fig. 2
$l, l_1$	= moment arms, see Fig. 2
$P_1, P_2, P_3$	= functions defined in Eqs. 9a,b,c
$q$	= uniform surcharge load
$r_o, r(\theta), \bar{r}_o(\bar{\theta}), r(\bar{\theta})$	= length variables of logarithmic spiral curve, see Fig. 4
$r'(\theta)$	= $dr/d\theta$
$S$	= slip surface
$u_1, u_2, u_3, u_4$	= functions defined in Appendix II
$W, W_1$	= weight of sliding mass, fictitious weight, see Fig. 2
$\sigma(\theta)$	= normal stress distribution along slip surface
$\tau(\theta)$	= tangential stress distribution along slip surface
$\gamma$	= unit weight of soil
$\varphi$	= friction angle of soil
$\lambda_1, \lambda_2, \lambda_3$	= constant parameters
$\theta_o, \theta_h, \bar{\theta}_o, \bar{\theta}_h$	= angular variables, see Fig. 4
$\beta$	= slope angle
$\alpha$	= angle defined in Eq. 7a and
$\xi$	= angle defined in Eq. 7b

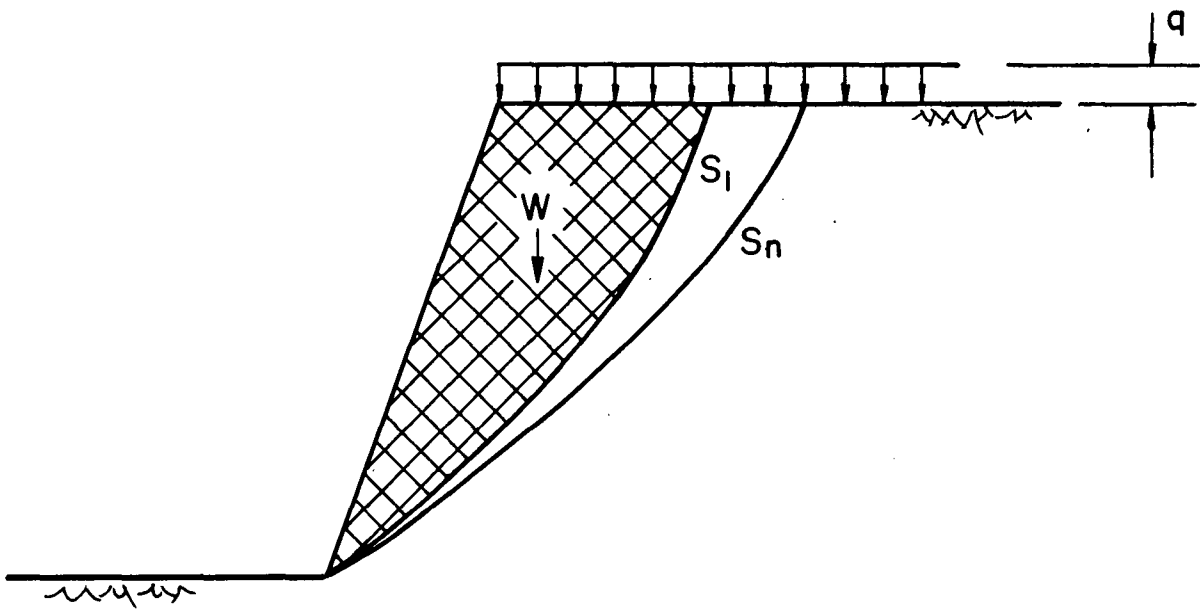


Fig. 1 Slope with Potential Slip Surfaces

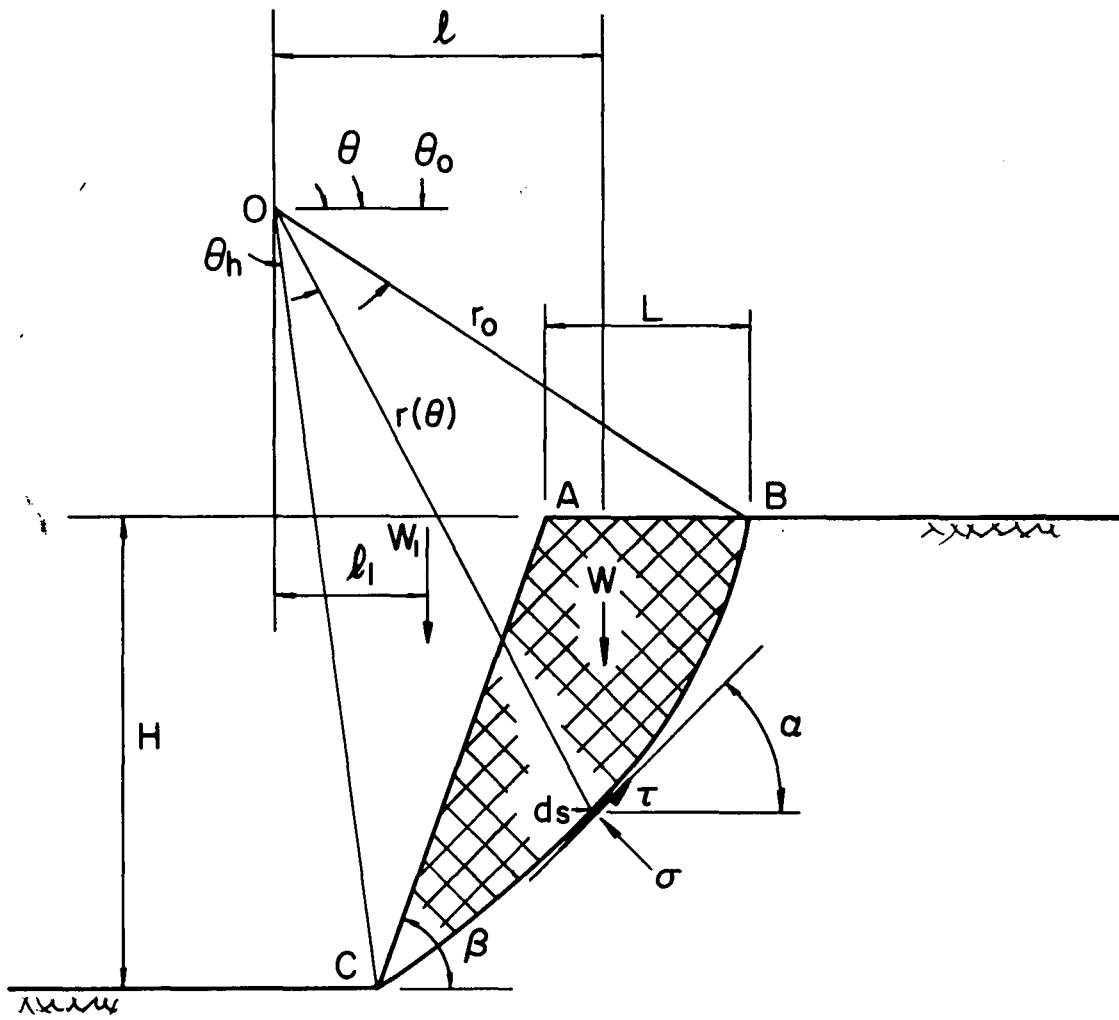
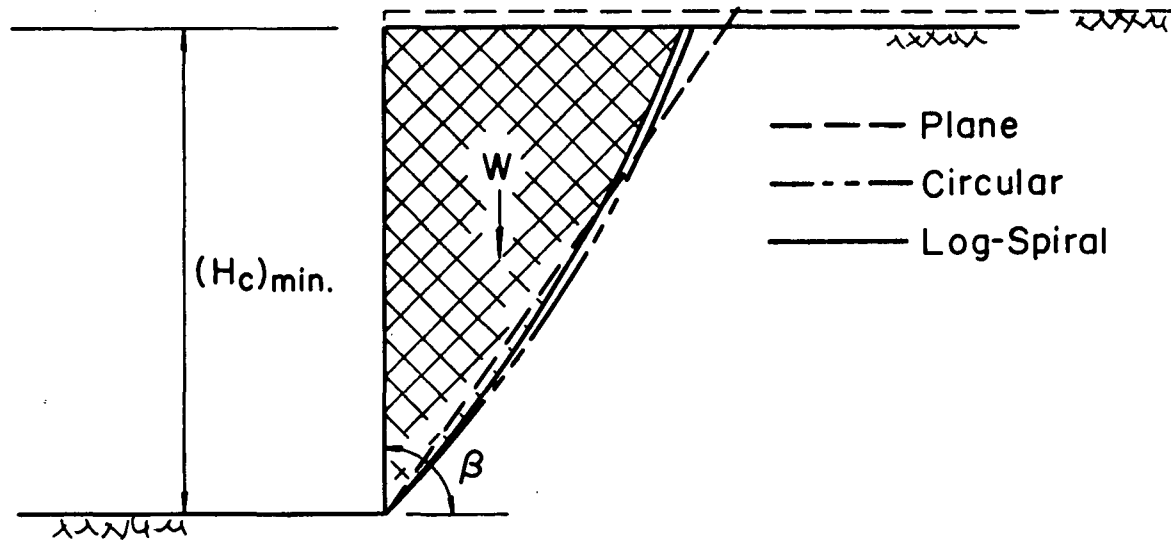
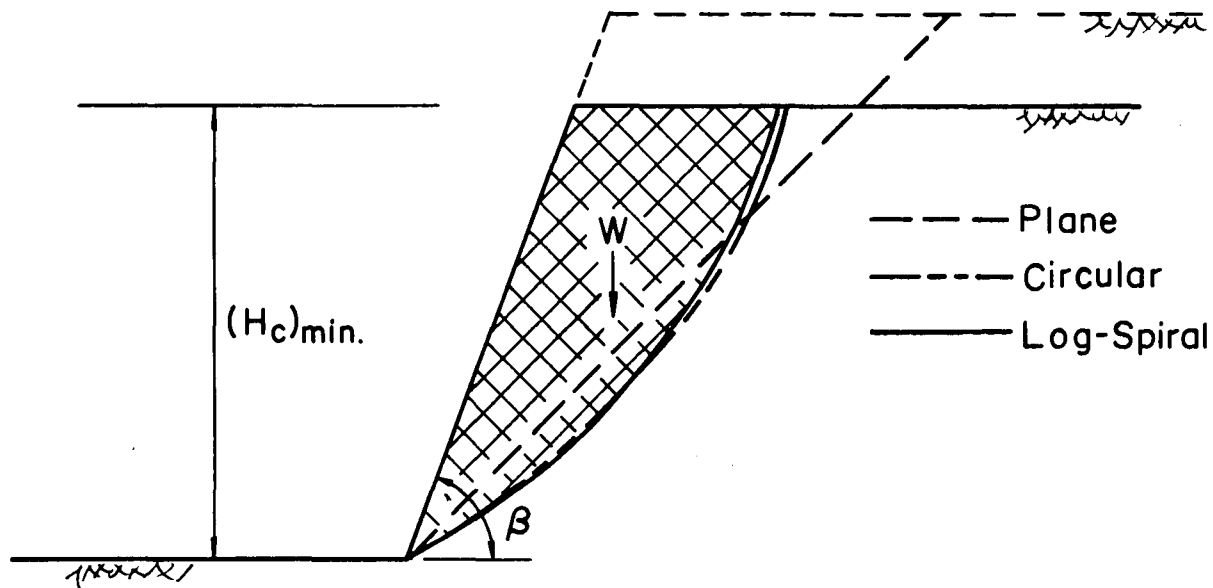


Fig. 2 Slope of Uniform Soil



a)  $\beta=90^\circ, \phi=20^\circ$



b)  $\beta=70^\circ, \phi=20^\circ$

Fig. 3 Comparison of Weights of the Sliding Mass for Different Slip Surfaces

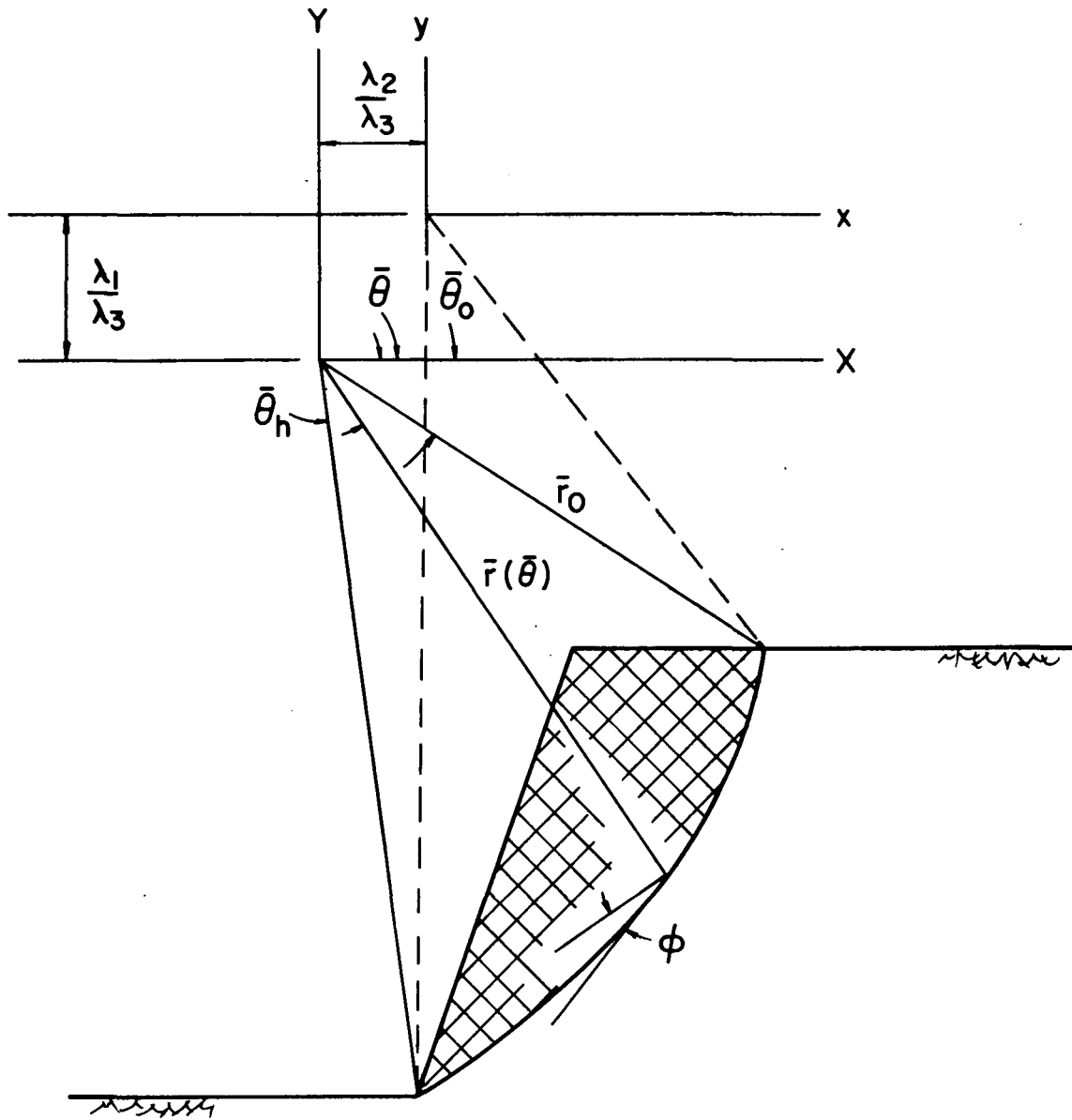
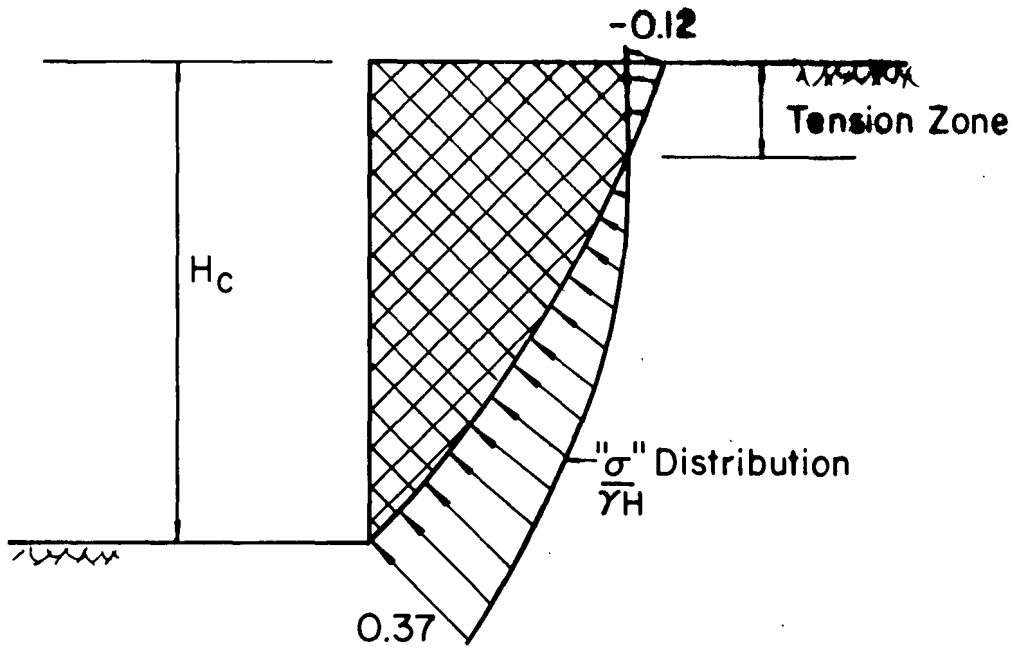
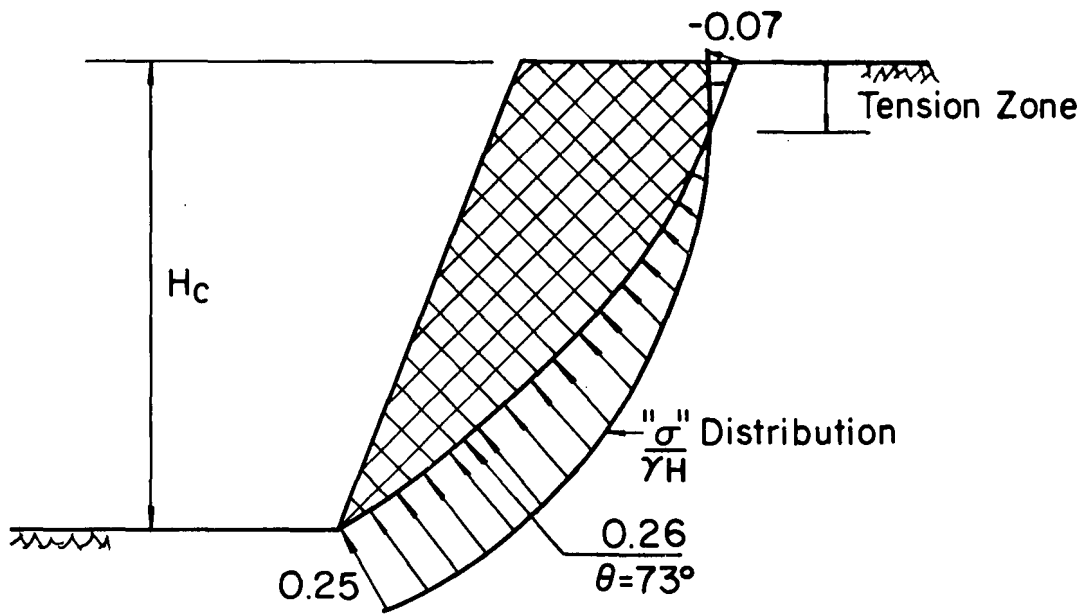


Fig. 4 Transformation of Coordinates



a)  $\beta=90^\circ, \phi=20^\circ$



b)  $\beta=70^\circ, \phi=20^\circ$

Fig. 5 Normal Stress Distribution